Manipulating Small Particles in Mixtures far from Equilibrium

Sergey Savel'ev,[1] Fabio Marchesoni,[1,2] and Franco Nori[1,3]

[1]*Frontier Research System, The Institute of Physical and Chemical Research (RIKEN), Wako-shi, Saitama, 351-0198, Japan*
[2]*Dipartimento di Fisica, Universitá di Camerino, I-62032 Camerino, Italy*
[3]*Center for Theoretical Physics, Department of Physics, University of Michigan, Ann Arbor, Michigan 48109, USA*

(Received 2 August 2003; published 23 April 2004)

The motion of two interacting species of small particles, coupled differently to their environment, is studied both analytically and via numerical simulations. We find three ways of controlling the particle motion of one (passive) B species by means of another (active) A species: (i) dragging the target particles B by driving the auxiliary particles A, (ii) rectifying the motion of the B species on the asymmetric potential created by the A-B interactions, and (iii) dynamically modifying (pulsating) this potential by controlling the motion of the A particles. This allows easy control of the magnitude and direction of the velocity of the target particles by changing the ac drive(s).

DOI: 10.1103/PhysRevLett.92.160602 PACS numbers: 05.40.–a

The manipulation of tiny particles, which are strongly influenced by their noisy environment, has required novel approaches to control their motion [1]. If small particles are driven by an ac external force on an asymmetric substrate, their ac motion can be rectified, thus providing useful work [1]. The interaction among particles diffusing through a ratchet has been neglected in theoretical studies (with the exception of very few special systems [2] or few numerical studies [3,4]). Indeed, as shown here, particle-particle interactions produce unusual dynamics.

Recent experiments on transport of K and Rb ions in an ion channel [5] and particles of different size in asymmetric silicon pores [6] pose the question of how directed motion of two or more species affect one another. More interestingly, one might wonder how to induce and control the net transport of passive particles, which are insensitive to the applied drives and/or substrates. A way to tackle this challenging problem is to employ auxiliary particles A that (i) interact with the target species (the B particles) and (ii) are easy to drive by means of external forces. By driving the auxiliary particles A one can regulate the motion of otherwise passive particles B through experimentally accessible systems, like ion channels [5], artificial pores [6,7], arrays of optical tweezers [8], or certain superconducting devices [4].

In order to study the influence of the interspecies interaction on particle transport in a binary mixture, we consider external forces applied either to the A particles only or simultaneously to both A and B species. We have found that (1) with increasing the intensity of an applied dc driving force, there is a dynamical phase transition from a "clustered" motion of A and B particles to a regime of weakly coupled motion; (2) by applying a time-asymmetric zero-mean drive to the A species only, we can obtain a net current for both the A and B species; (3) when two ac signals $f_A(t)$ and $f_B(t)$ act independently on the A and B particles, respectively, and the A particles feel the asymmetric substrate, we can deliver these two species in the same or opposite direction by changing the relative phase of the signals $f_A(t)$ and $f_B(t)$ for both attractive and repulsive A-B interactions. Systems where our two-species transport technique might be useful are the focus of ongoing experimental work (e.g., superconducting samples penetrated by topologically different vortices [9], ion channels with different ions [5]).

Model.—We consider transport in quasi-one-dimensional geometries, thus including the wide category of fabricated devices and nanobiological systems addressed in the recent ratchet literature [10]. Since the dragging effect implies "trapping" the target species B by another species A, we need first to take into account the local change in the distribution of B particles near an A particle. This can be done by considering the binary distribution function $F_{AB}(x, x')$, which describes the probability of finding an A particle near x and a B particle near x'. A partial differential equation for F_{AB} can be constructed by averaging the time derivative of the microscopic binary distribution $N_{AB} = \sum_{i,j} \delta[x - x_{A,i}(t)] \times \delta[x' - x_{B,j}(t)]$ over different stochastic realizations. Here, the sum has to be taken over the coordinates $x_{A,i}$ and $x_{B,j}$ of all the A and B particles at time t. As the main goal of this paper is to study the behavior of one species relative to the other, we further neglect the interaction among particles of the same type. This simplification, reminiscent of the so-called "color charge" scheme for binary colloidal mixtures [11], does not appreciably affect our major conclusions [see discussion of Fig. 1(a)].

The relevant Langevin equations are $dx_{a,i}/dt = -\partial/\partial x_{a,i}[U_a + \sum_{j,j'} W(x_{A,j} - x_{B,j'})] + \sqrt{2T}\xi_a^{(i)}$, where T is the temperature, $\xi_a^{(i)}$ are white noises with $\langle \xi_a^{(i)} \rangle = 0$, $\langle \xi_a^{(i)}(t) \xi_b^{(j)}(0) \rangle = \delta_{a,b}\delta_{i,j}\delta(t)$, and $a, b = A$ or B, and $W(x_{A,j} - x_{B,j'})$ denotes the interaction between the jth A particle and the j'th B particle. We assume that the A species is driven by the time-dependent force $f_A(t)$, possibly in the presence of a periodic asymmetric substrate $U_{\rm as}(x)$ with period l, say $U_{\rm as}(0 < x < l_1) = Q\,x/l_1$, $U_{\rm as}(l_1 < x < l) = Q(l - x)/(l - l_1)$, and $Q \geq 0$, while the B species is not subject to an asymmetric substrate

but only to the external force $f_B(t)$; namely, $U_A = U_{as} - f_A(t)\,x$, and $U_B = -f_B(t)\,x$. The Langevin equations can be manipulated to determine the time evolution of F_{AB} at B densities n_B much lower than the A density n_A:

$$\partial_t F_{AB} = \partial_x\{F_{AB}\partial_x\mathcal{E}_A + T\partial_x F_{AB}\} + \partial_{x'}\{F_{AB}\partial_{x'}\mathcal{E}_B + \int dx'' F_{ABA}(x, x', x'')\partial_{x'}W(x' - x'') + T\partial_{x'}F_{AB}\}, \quad (1)$$

where $\mathcal{E}_A = U_A(x) + W(x - x')$, $\mathcal{E}_B = U_B(x') + W(x - x')$, and $F_{ABA}(x, x', x'')$ is the three-particle distribution function related to the probability of finding two A particles in x and x'' and a B particle in x'. Hereafter, $\partial_t = \partial/\partial t$ and $\partial_x = \partial/\partial x$.

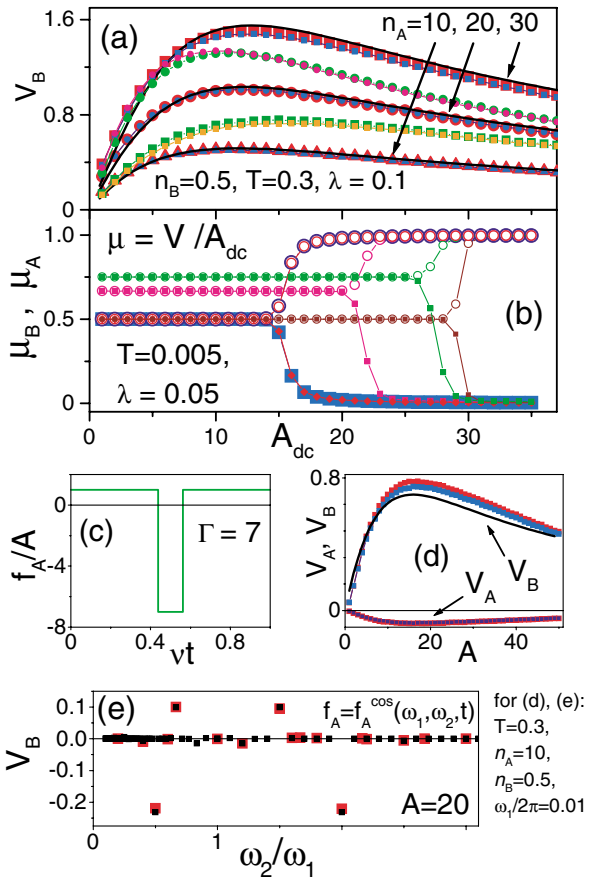

FIG. 1 (color). Dragging particles B by auxiliary particles A in the case of no substrate, $U_{as} = 0$, and interaction strength $g = \pm 0.02$. (a) Symbols are from molecular dynamics (MD) simulations (red and blue symbols for repulsive and attractive A-B interactions, respectively) with time step $dt = 47 \times 10^{-5}$; black lines are the results of analytical calculations. The green/magenta and olive/orange symbols are data for $n_A = 40$, $g = \pm 0.02$ and nonzero interactions between the same particles $g_a = 0.01/-0.005$. (b) The mobility of A and B particles versus dc force A_{dc} obtained from the MD simulations for lower temperature and repulsive interactions. The different numbers of particles in a cluster are chosen as $(N_A, N_B) = (1, 1)$ red, (2,2) brown, (2,1) magenta, (3,1) green. For comparison, the case of attractive interaction and $(N_A, N_B) = (1, 1)$ is shown in blue. Open (filled) symbols refer to active (passive) particles. (d),(e) The net velocities V_A and V_B, from MD, versus driving amplitude A (d) or frequencies ω_2/ω_1 (e) for $\lambda = 0.075$. The time-asymmetric signal used in (d) is shown in (c). Red and blue symbols in (d) correspond to repulsive and attractive interactions. The black line in (d) and black squares in (e) represent V_B calculated analytically.

Next, we express F_{ABA} in terms of one-particle F_a and binary distribution F_{AB} functions. In general, a binary function can be written as $F_{AB}(x, x') = F_A(x)F_B(x') \times G[(x + x')/2, x - x']$ where F_A and F_B are the one-particle distributions for A and B and G defines the deviation of the distribution of the A particles near a B particle. Thus, the three-particle distribution can be expressed as $F_{ABA}(x, x', x'') = F_B(x')F_A(x)G[(x + x')/2, x - x'] \times F_A(x'')G[(x' + x'')/2, x'' - x']$. We also consider the interaction range λ of the A-B interactions to be much smaller than l. In such a case we can assume long distances $|x - x'| \gg \lambda$ (where $G[(x + x')/2, x - x'] = 1$) in order to derive F_A and F_B, and short distances $|x - x'| \leq \lambda$ to calculate G. In the long distance limit, we obtain the Fokker-Planck equations for F_A and F_B:

$$\begin{aligned} F_A\partial_x U_A + T\partial_x F_A &= -j_A, \\ F_B(\partial_x[U_B + gF_A] + \beta F_A) + T\partial_x F_B &= -j_B \end{aligned} \quad (2)$$

with effective interaction constant $g(x) = \int dy W(y) \times G(x, y)$ and dragging coefficient $\beta(x) = \int dy W(y)\partial_y \times G(x, y) - \partial_x g(x)/2$. The particle currents j_a are defined by $\partial_t F_a = -\partial_x j_a$ and, in the adiabatic approximation studied below, depend on the instantaneous value of the driving forces $f_a(t)$. The equation for the correcting factor $G(x, y)$ can be easily constructed by imposing $|y| \lesssim \lambda \ll l$ in Eq. (1). For simplicity, we display only the case when $U_{as} = 0$, i.e.,

$$\partial_y\{G[\partial_y W(y) - V_{AB}] + T\partial_y G\} = 0, \quad (3)$$

where $V_{AB} \equiv V_A - V_B = j_A/n_A - j_B/n_B$ is the relative velocity. Therefore, the A-B interaction produces (1) an effective potential $g(x)F_A$ acting on the B particles, which were originally insensitive to the substrate, and (2) an effective drag βF_A exerted by the As on the Bs.

We concentrate now on three potential applications to transport control in microdevices that allow an instructive comparison between analytical solutions and numerical simulations of a driven binary mixture.

Dragging by auxiliary particles.—When no force acts on the B species, the dc-driven A particles can drag along the B particles. When $U_{as} = 0$ [Eq. (3)], the dragging problem (with $f_B = 0$ and $f_A = A_{dc}$) is solved analytically. If $j_A = j_B = 0$, the function G is a simple Boltzmann distribution $G = \exp(-W/T)$, while if $V_A > 0$ one obtains $G = (V_{AB}/2T)\int_y^\infty dz \exp\{[W(z) - W(y) - V_{AB}(z - y)/2]/T\}$. Inserting G in Eq. (2) yields $V_A = f_A$, $V_B = n_A \int dy G(y)\partial_y W$. Next, we performed numerical simulations of the Langevin equations for the A and B

particles with $W(y) = g(\lambda - |y|)/\lambda^2$, if $|y| < \lambda$, and $W = 0$ otherwise. In spite of the finite interaction length λ introduced in our simulation, the analytical equation for V_B obtained above describes fairly closely our data in Fig. 1(a), showing that the dragging effect attains a maximum for a certain value of A_{dc}. Introducing the pair interaction between the particles of the same type $W_a(y) = g_a(\lambda - |y|)/\lambda^2$ if $|y| < \lambda$ and $W_a = 0$ otherwise, we found a similar dependence of V_B on A_{dc} [see Fig. 1(a)] also outside the "color charge" scheme. With decreasing temperature, the solution of the derived transcendental equation for V_B vanishes, signaling the occurrence of a dynamical phase transition. Indeed, for weak driving forces, all A and B particles tend to cluster together. In order to estimate both the maximum driving force A_{dc}^{crit} for the clusters to be stable and their translational velocity V_{clust}, we introduce force-balance equations for clustered N_A A and N_B B particles at $T = 0$: $V_A = V_{clust} = f_A - N_B f_{int}$; $V_B = V_{clust} = N_A f_{int}$ with interaction force $f_{int} \le \max|\partial_y W| = |g|/\lambda^2$. Thus, we obtain $V_{clust} = N_A f_A/(N_A + N_B)$ for a dc driving force $A_{dc} < A_{dc}^{crit}$ and $A_{dc}^{crit} = (N_A + N_B) \cdot \max|\partial_y W|$. This gives the cluster mobility $\mu_{clust} = V_{clust}/A_{dc} = 1/2,\ 1/2,\ 2/3,\ 3/4$ and critical force $A_{dc}^{crit}(|g| = 0.02, \lambda = 0.05) = 16,\ 32,\ 24,\ 32$ for clusters with $(N_A, N_B) = (1,1), (2,2), (2,1), (3,1)$, respectively. These numbers are in good agreement with simulation results of Fig. 1(b).

Rectifying the ac dragging.—The dragging effect may be used to induce a net motion of both A and B particles in the absence of a substrate, $U_{as} = 0$: As an additional ingredient, a time-asymmetric zero-average force [like the sinusoidal force $f_A(t) = f_A^{\cos}(\omega_1, \omega_2) = A(\cos\omega_1 t + \cos\omega_2 t)$ with $\omega_2 = 2\omega_1$, or the rectangular waveform of Fig. 1(c)] must be applied to one species, say, the auxiliary particles A. Indeed, applying the alternate signals $f_A = -\Gamma A$ and $f_A = A$, during the time intervals $t_1 = 1/(1+\Gamma)\nu$ and $t_2 = \Gamma/(1+\Gamma)\nu$, respectively, forces time-periodic particle flows with frequency ν. The net B current can be written as $\langle V_B \rangle_t = [V_B(f_A = \Gamma A) + \Gamma V_B(f_A = -A)]/(1+\Gamma)$ with time-asymmetry factor Γ. The average $\langle V_B \rangle_t$ can be easily calculated through our analytical expression for the thermally averaged V_B as well as from simulations; data and analytical results compare very well [Fig. 1(d)]. The rectification due to the A-B dragging can also be seen as spikes or resonances [Fig. 1(e)] on the dependence of the net velocities V_B and V_A on the frequency ω_2, if the signal $f_A = f_A^{\cos}(\omega_1, \omega_2)$ with two frequencies is applied. When changing ω_2/ω_1, the change of the sign of the net velocities allows one to effectively control the motion of both species.

Rectification via the effective potential created by the auxiliary particles.—If the A particles move on an asymmetric substrate, the equation for G becomes complicated. Thus, we will now consider a mean-field (MF) approximation when $G = 1$ [12]. Even though dragging is lost in such an approximation ($\beta = 0$), the effective potential acting upon the target B particles can be

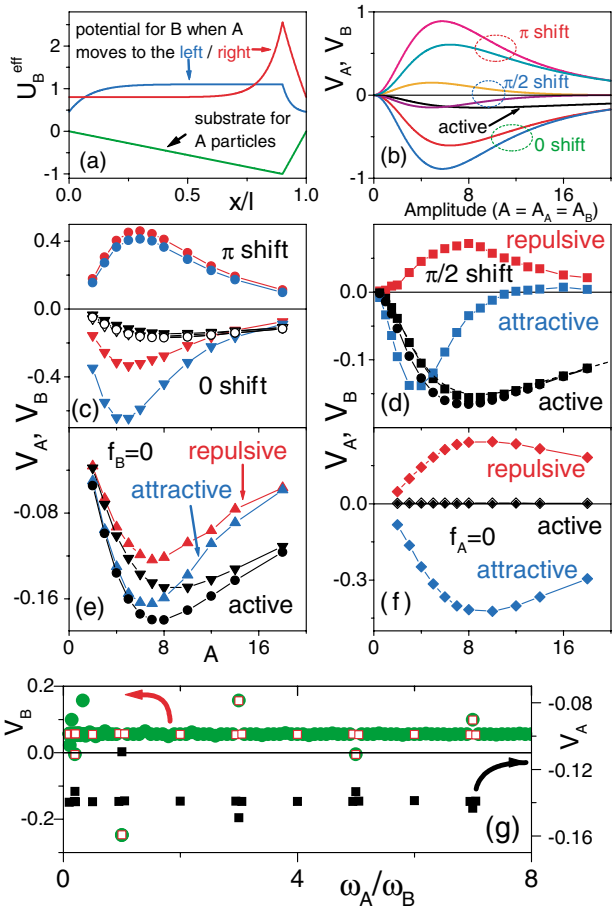

FIG. 2 (color). How to control the net velocities V_A, V_B by ac forces f_A and f_B on an asymmetric substrate potential [green profile in (a)] coupled to the A particles, only. We set $\lambda = 0.075$, $n_A = 50$, $n_B = 1$, $dt = 0.00047$, $|g| = 0.02$, $Q = -1$, $l_1 = 0.9$, and $T = 0.6$. (a) The effective MF potential (red and blue landscapes) felt by the B particles when the A particles are forced towards the "hard" (to the right) or to the "easy" (to the left) directions, respectively. (b) V_A and V_B versus the ac amplitude A of f_A and f_B calculated in the MF approximation for the repulsive/attractive A-B interaction and in-phase (red/blue), out-of-phase (pink/light blue), and $\pi/2$-shifted (orange/violet) ac forces. (c) The MD data of V_B for repulsive/attractive species and in-phase (red/blue triangles) and opposite-phase (red/blue circles) driving forces; black symbols mark V_A. (d) The same as in (c) with red/blue squares for repulsive/attractive interactions and $\pi/2$-shifted ac forces; black symbols are V_A. (e) The ac force is applied only to the A species (i.e., $f_B = 0$). V_B is marked by red/blue up triangles for repulsive/attractive interactions, the corresponding V_A marked by down triangles/circles. (f) The ac force is applied only to B particles ($f_A = 0$), V_A is very weak (black symbols), but the ac motion of B particles is rectified by an effective asymmetric potential (V_B is plotted by red/blue symbols for repulsive/attractive interactions). (g) The dependence of the net velocities V_A (black squares from MD) and V_B (red open symbols from MD and green filled circles calculated analytically and linearly scaled to fit MD data) on the frequency ratio ω_B/ω_A (odd rations provide peaks) for repulsive interactions and $A_A = A_B = 8$, $\phi_A = \phi_B = 0$.

qualitatively reproduced. In the adiabatic approximation [1] Eqs. (2) yield for the net current of the a species $J_a = \int_0^{1/\nu} dt j_a[f_A(t), f_B(t)]$ with $j_a = n_a l T[1 - \exp(-l f_a/T)]/\int_0^l dx \int_x^{x+l} dz \exp([U_a^*(z) - U_a^*(x)]/T)$, where $U_A^* = U_A$ and $U_B^*(x, f_A, f_B) = g_{\rm MF} F_A(x, f_A) - f_B x$ with $g_{\rm MF} = \int dy W(y)$. The polarity (or asymmetry) of $g_{\rm MF}F_A$ coincides with the polarity of the original substrate $U_{\rm as}$ for attractive interaction, $g_{\rm MF} < 0$, and vice versa for repulsive A-B potentials, $g_{\rm MF} > 0$. Therefore, the ac motion of B particles can be rectified on this potential ("mediated" ratchet effect). However, there is an additional effect controlling the B motion as the effective potential $g_{\rm MF}F_A$ changes with time. When the force $f_A(t)$ points against the steeper substrate slopes (the "hard-motion direction"), the A particles tend to accumulate near the $U_{\rm as}$ minima. Thus, due to the repulsive (attractive) A-B interactions, this strongly nonuniform distribution of A particles causes high peaks (deep wells) in the effective potential acting on the B particles [Fig. 2(a)]. The ensuing high potential barriers of $U_B^{\rm eff}$ significantly slow down the B particle motion (gating effect) when the A particles move in their "hard" direction. In contrast, the relatively faster motion of the A particles as $f_A(t)$ pushes them in the opposite, "easy" direction, corresponds to shallower $U_B^{\rm eff}$ barriers and, thus, to a higher B mobility.

An example.—Let us consider ac drives of the form $f_A(t) = A_A \mathrm{sgn}[\cos(\omega_A t + \phi_A)]$ and $f_B(t) = A_B \mathrm{sgn}[\cos(\omega_B t + \phi_B)]$ with $\mathrm{sgn}[\cdots]$ denoting the sign of the argument. If the frequencies and amplitudes of both signals coincide $\omega_A = \omega_B = \omega$, $A_A = A_B = A$, we can restrict the discussion to three main cases depending on the relative phase of the ac forces: (i) in-phase drives: $\phi_A = \phi_B$; (ii) opposite-phase drives: $\phi_A = \phi_B + \pi$; and (iii) $\pi/2$-shifted drives: $\phi_A = \phi_B + \pi/2$. In the first two cases the gating effect is dominant and the direction of the B current does not depend on the polarity of $g_{\rm MF}F_A$, i.e., the sign of V_B is insensitive to the sign of the A-B interactions (attractive or repulsive). Indeed, the A particles, when pushed against the steeper slopes of $U_{\rm as}$, create the high barriers of $U_B^{\rm eff}$ [Fig. 2(a)] that lock the motion of B particles as long as f_B pushes them to the right or to the left in the case of in-phase or opposite-phase ac drives. Thus, the A and B particles drift necessarily to the same or opposite direction for cases (i) or (ii), respectively. In contrast, when $f_A(t)$ and $f_B(t)$ are phase shifted by $\pi/2$, the B particle motion is governed by the asymmetry of the effective potential $g_{\rm MF}F_A$. During the half ac cycle when the effective potential $U_B^{\rm eff}$ develops high (low) barriers, the B particles are being pushed directly by $f_B(t)$ to the right and to the left for the same amount of time. Thus, the B particles are driven back and forth on the asymmetric ratchet potentials $g_{\rm MF}F_A(x, f_A = A)$ and $g_{\rm MF}F_A(x, f_A = -A)$, alternately. Since the polarity of these potentials depends on the sign of the interaction $g_{\rm MF}$, attracting A and B particles move together $[\mathrm{sgn}(J_A) = \mathrm{sgn}(J_B)]$, while repelling particles travel in opposite directions $[\mathrm{sgn}(J_A) = -\mathrm{sgn}(J_B)]$. Examples of MF calculations for in-phase, opposite-phase, and $\pi/2$-shifted drives are shown in Fig. 2(b). Our numerics prove that dragging effects may correct the MF estimates of V_B, so as to break the symmetry with respect to the interaction sign [see Fig. 2(c) for cases (i) and (ii) and Fig. 2(d) for (iii)]. Nevertheless, the main MF picture remains valid. In order to clearly separate dragging and rectification effects, we performed simulations with $A_A \neq 0$, $A_B = 0$ [Fig. 2(e)] and with $A_A = 0$, $A_B \neq 0$. For the first case (dragging), the A and B particles drift in the same direction, while in the second case (mediated ratchet) the sign of V_B is determined by the sign of the A-B interactions. Finally, if we fix amplitudes and phases, for instance, $A_A = A_B$ and $\phi_A = \phi_B$, and change the frequency ratio ω_A/ω_B, we obtain velocity spikes for commensurate values of ω_A and ω_B. Indeed, in the incommensurate case the gating effect is irrelevant and the net motion is determined by a combination of mediated ratchet and dragging effect. However, if the frequencies of the driving signals are commensurate, the modulation of the effective potential $U_B^{\rm eff}$ gets time correlated with the direct ac drive $f_B(t)$, thus resulting in large deviations of V_B from its incommensurate baseline [see Fig. 2(g)]. Note that spikes happen at different winding numbers for the cases shown in Figs. 1(e) and 2(g).

The effects presented here can be potentially useful for particle motion control in a variety of different systems. Examples include new types of superconducting devices with different species of vortices [9], for spin-separating nanodevices, for ion mixtures traveling through cell membranes [5] or moving through artificial nanopores [7], for controlling transport in colloidal suspensions [8], and for particle-size separation.

We gratefully acknowledge support from the U.S. NSF Grant No. EIA-0130383. F. M. thanks the Canon Foundation for financial support.

[1] P. Reimann, Phys. Rep. **361**, 57 (2002); R. D. Astumian and P. Hänggi, Phys. Today **55**, No. 11, 33 (2002).
[2] F. Marchesoni, Phys. Rev. Lett. **77**, 2364 (1996); P. Reimann *et al.*, Europhys. Lett. **45**, 545 (1999).
[3] I. Derényi and T. Vicsek, Phys. Rev. Lett. **75**, 374 (1995).
[4] B. Y. Zhu *et al.*, Phys. Rev. B **68**, 014514 (2003).
[5] J. H. Morais-Cabral *et al.*, Nature (London) **414**, 37 (2001).
[6] S. Matthias and F. Muller, Nature (London) **424**, 53 (2003).
[7] Z. Siwy and A. Fuliński, Phys. Rev. Lett. **89**, 198103 (2002); C. Marquet *et al.*, *ibid.* **88**, 168301 (2002).
[8] P. T. Korda *et al.*, Phys. Rev. Lett. **89**, 128301 (2002); B. A. Koss and D. G. Grier, Appl. Phys. Lett. **82**, 3985 (2003).
[9] S. Savel'ev and F. Nori, Nature Materials **1**, 179 (2002).
[10] See, e.g., H. Linke, Appl. Phys. A **75**, No. 2 (2002).
[11] W. G. Hoover *et al.*, Phys. Rev. E **57**, 3911 (1998).
[12] S. Savel'ev *et al.*, Phys. Rev. Lett. **91**, 010601 (2003).